Field Theoretical Computer-Aided Design of Rectangular and Circular Iris Coupled Rectangular or Circular Waveguide Cavity Filters

Uwe Papziner and Fritz Arndt, *Fellow, IEEE*

***Abstract*— The rigorous CAD of a class of rectangular and circular waveguide cavity-filters is described which are coupled by rectangular and/or circular irises. The design theory is based on the full wave mode-matching method for three key-building block elements (asymmetric rectangular double-step, asymmetric rectangular-to-circular and circular-to-circular waveguide junction) associated with the generalized S-matrix technique for the composite structures. The waveguide filters may be arbitrarily composed of the key-building block elements and the rectangular or circular waveguide sections between them. Finite iris thicknesses, higher order mode interactions, as well as asymmetric structures are rigorously taken into account. The theory is verified by measurements.**

I. Introduction

IRIS COUPLING [1]–[29] of waveguide half-wave resonators is a well proven technique to produce waveguide bandpass filters for a large variety of applications, such as for components of composite filters and multiplexers with high rejection requirements, [3], [12], [13]–[15], [19], [29], for filters at high input power levels, [13], [15], or for satellite communication systems [13], [19], [21], [22]. Although many refined design procedures are available which are based on improved equivalent circuit models, [3]–[7], [14], [15], the continued development of communication systems with more stringent passband and stopband control, and the increasing activity at millimeter-wave frequencies with tight mechanical tolerances, have stimulated advances in rigorous field theoretical methods which allow accurate computer-aided filter design taking into account both the finite thickness of the irises and the higher order mode interaction between the discontinuities. Moreover, with the growing demand for such components to be applied for integrated circuits purposes, such as for multiplexers or receiver front-ends, [12], [13], [19], [29] the inclusion of higher-order mode coupling effects between the individual parts becomes increasingly important for the design of compact structures.

For the case of small irises and thin walls, the coupling coefficients are available in form of approximate formulas [1]–[5], [23]–[26]; large irises and finite wall thicknesses may be treated by correction factors, [6], [7], [14]. Field theoretical analyses have been reported for the rectangular, circular or rectangular-to-circular waveguide step discontinuity alone, [9]–[11], [16]–[18], [31]–[32], for single rectangular or circular waveguide irises [6], [9]–[11], [16]–[18], for rectangular waveguides periodically loaded with irises [8], [9], for the rigorous design of inductive or capacitive iris coupled filters [21], [22], and the analysis of rectangular waveguides loaded with symmetric capacitive or rectangular irises by an efficient modified TE_{mn}^{X} wave approach [20]. A complete field theory treatment of the class of filters shown in Fig. 1, however, has not yet been presented where the waveguide structures may be arbitrarily composed of rectangular and circular waveguide elements.

The purpose of this paper is, therefore, to extend the mode-matching description given in [8]–[11], [16]–[22] to the new aspect that rectangular or circular cavity filters coupled by circular and/or rectangular irises (Fig. 1) may be included in the general, rigorous and efficient field-theory based computer-aided design procedure which has hitherto been applied merely for the case of rectangular [10], [20], [34] or inductive iris [21] coupled rectangular cavity filters. Moreover, since higher-order mode coupling effects are rigorously taken into account, also interactions between different modes of operation in the cavities may be expressed in a form suitable for computer-aided design.

Based on the old idea to use different waveguide cavities [33], improved rejection requirements may be met by the modified designs shown in Figs. 1(b), (d), (e), i.e. with increased-width resonator sections, with combined rectangular and circular waveguide structures, as well as by designs utilizing asymmetric irises. This is mainly due to suitably altered fundamental mode cutoff frequencies in the resonator sections and to interactions with higher-order modes. The additional junction effects may advantageously be utilized in the optimization process as extra design parameters.

The design method proposed is based on the full wave mode-matching method for three general key-building block elements (rectangular double-step, rectangular-to-circular and circular-to-circular waveguide junction) associated with the generalized S-matrix technique for composite structures. The waveguide structures may then be arbitrarily composed of the key-building block elements and homogeneous waveguide sections between them. Finite iris thicknesses, higher order mode interactions at all step discontinuities, as well as asymmetric structures are rigorously taken into account.

For the derivation of the modal S-matrix of the key-building block elements only the inversion of a submatrix with a

Manuscript received March 19, 1992; revised July 9, 1992.

The authors are with the Microwave Department, University of Bremen, Kufsteiner Str., NW1, D-2800 Bremen, Germany.

IEEE Log Number 9205461.

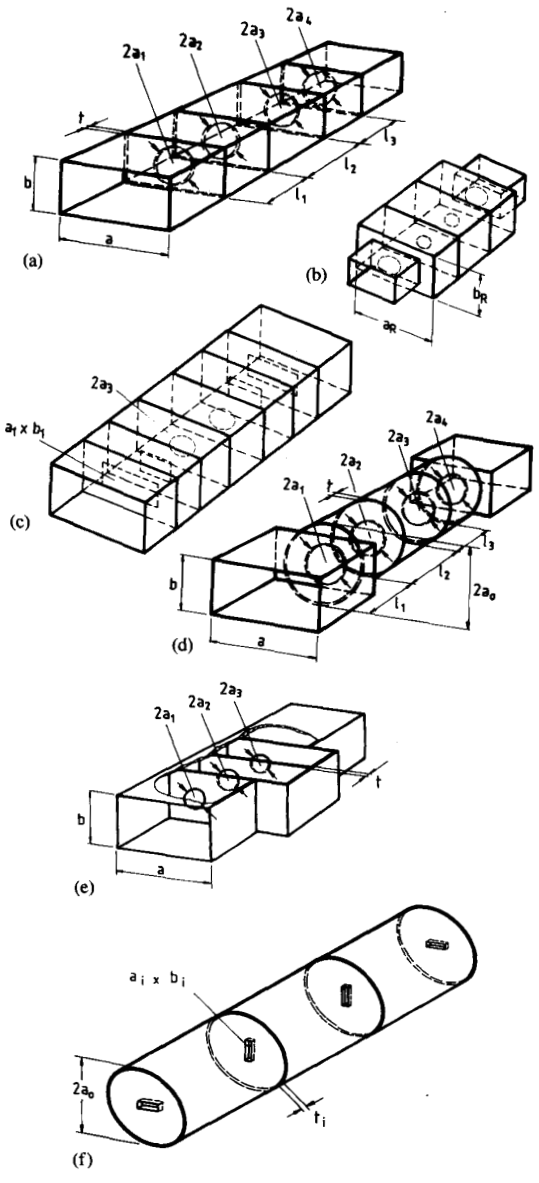

Fig. 1. Investigated class of rectangular and circular waveguide cavity filters coupled by rectangular and/or circular irises: (a) Circular iris coupled rectangular waveguide resonators. (b) Circular iris coupled rectangular waveguide resonators of increased width. (c) Rectangular and circular iris coupled rectangular waveguide resonators. (d) Circular iris coupled circular waveguide resonators with rectangular waveguide instrumentation. (e) Asymmetric circular iris coupled rectangular waveguide resonators. (f) Rectangular iris coupled circular waveguide resonators.

quarter of the size of the original matrix of the coupling integrals is required as the modified algorithm of [29], [30] is utilized. Furthermore, a suitable sub-cascading technique for discontinuities of extreme step heights or widths, and an implicit mode selection process for each individual step junction, help to circumvent relative convergence problems as well as to reduce the number of modes. Moreover, the asymmetric modal S-matrix formulation for the key-building block elements used leads to a significant reduction of the total computational effort, since there is no need to maintain the number of "localized" modes [8], necessary for calculating the scattering matrix of the iris, with the relatively long homogeneous cavity section between them where only a few "accessible" modes [8] (the propagating modes and a the first few evanescent ones) may be sufficient.

An optimizing computer program varies the filter parameters until passband and stopband insertion loss correspond to predicted values. Computer-optimized examples demonstrate the efficiency of the presented method. The theory is experimentally verified by available examples.

II. Theory

For the rigorous computer-aided design of the filter structures to be investigated (Fig. 1), the full wave mode-matching method is applied for a few key-building block elements associated with the generalized S -matrix technique for composite structures. Three key-building block elements are required to include all general cases under consideration (Figs. 1): The asymmetrical rectangular double-step [10], [32], the rectangular-to-circular [9], [17], and the circular-to-circular waveguide junction [18], [31]. Note that for the corresponding inverse discontinuities merely the corresponding modal S-matrix needs to be transposed [10].

For the derivation of the mode-matching method for the key-building blockelements, the reader is referred to the literature. However, for completeness it seems to be convenient to present the main steps of the derivation for the modal S-matrix of the rectangular-to-circular waveguide junction at this place by using the full wave mode matching method in the current form which includes the general asymmetric case (Fig. 2(a)) required for calculating the asymmetric filter structure of e.g. Fig. 1(e).

For the waveguide subregion ν under consideration (cf. Fig.2(a)), the fields [23]

$$\begin{aligned}\vec{E}^{\nu} &= \nabla \times \nabla \times \vec{\Pi}_e^{\nu} - j\omega\mu\nabla \times \vec{\Pi}_h^{\nu} \\ \vec{H}^{\nu} &= j\omega\epsilon\nabla \times \vec{\Pi}_e^{\nu} + \nabla \times \nabla \times \vec{\Pi}_h^{\nu}\end{aligned} \tag{1}$$

are derived from the z components of the electric and magnetic Hertzian potentials $\vec{\Pi}_e, \vec{\Pi}_h$, respectively,

$$\begin{aligned}\vec{\Pi}_{ez}^{\nu} = &\sum_{(i,j)} \\ &\pm \left(\underline{a}_{(ij)}^{\nu} e^{-\underline{\gamma}_{(ij)}^{\nu} z} - \underline{b}_{(ij)}^{\nu} e^{+\underline{\gamma}_{(ij)}^{\nu} z}\right) \\ &\cdot T_{(ij)}^{\nu} \frac{-j}{\omega\epsilon_{\nu}\sqrt{\underline{Z}_{f(ij)}^{\nu}}}\end{aligned} \tag{2a}$$

$$\begin{aligned}\vec{\Pi}_{hz}^{\nu} = &\sum_{[m,n]} \\ &\pm \left[\underline{a}_{[mn]}^{\nu} e^{-\underline{\gamma}_{[mn]}^{\nu} z} + \underline{b}_{[mn]}^{\nu} e^{+\underline{\gamma}_{[mn]}^{\nu} z}\right] \\ &\cdot T_{[mn]}^{\nu} \frac{-j\sqrt{\underline{Z}_{f[mn]}^{\nu}}}{\omega\mu_{\nu}}\end{aligned} \tag{2b}$$

where $a_{(ij)}, b_{(ij)}, a_{[mn]}, b_{[mn]}$ are the still unknown eigenmode amplitude coefficients of the forward $(-)$ and backward (+) waves in z direction, (ij) stands for the TM and $[mn]$ for the

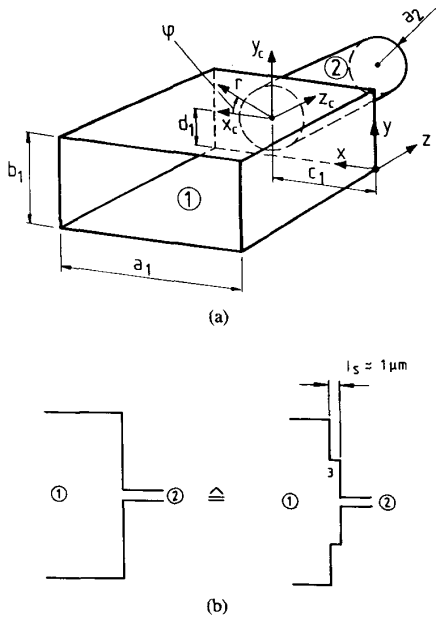

Fig. 2. Mode-matching method. (a) Key-building block discontinuity asymmetric rectangular-to-circular waveguide junction. (b) Artificial intermediate sections of zero or extremely small lengths forcalculating discontinuities of extreme step heights or widths.

TM modes, γ is the propagation factor of each mode, Z_f are the wave impedances

$$Z^{\nu}_{f(ij)} = \underline{Z}^{\nu}_{Fe} = \frac{\underline{\gamma}^{\nu}_{e}}{j\omega\epsilon_{\nu}}$$
$$Z^{\nu}_{f[mn]} = \underline{Z}^{\nu}_{Fh} = \frac{j\omega\mu_{\nu}}{\underline{\gamma}^{\nu}_{h}} \tag{3}$$

and T are the cross-section eigenfunctions of the rectangular (re) or circular (ci) waveguide section, respectively,

$$T^{re\,\nu}_{(ij)} = \frac{2\sin k^{\nu}_{x}x \sin k^{\nu}_{y}y}{k^{\nu}_{c}\sqrt{a_{\nu}b_{\nu}}} \tag{4a}$$

$$T^{re\,\nu}_{[mn]} = \frac{2\cos k^{\nu}_{x}x \cos k^{\nu}_{y}y}{k^{\nu}_{c}\sqrt{a_{\nu}b_{\nu}}\sqrt{1+\delta_{0m}}\sqrt{1+\delta_{0n}}} \tag{4b}$$

$$T^{ci\,\nu}_{(ij)} = \frac{J_i\left(\frac{x_{ij}}{a_{\nu}}r\right)\cdot\begin{pmatrix}\cos i\varphi\\ \sin i\varphi\end{pmatrix}}{x_{ij}\cdot J'_i(x_{ij})} \cdot\sqrt{\frac{2}{\pi(1+\delta_{0i})}} \tag{5a}$$

$$T^{ci\,\nu}_{[mn]} = \frac{J_m\left[\frac{x'_{mn}}{a_{\nu}}r\right]\cdot\begin{bmatrix}\cos m\varphi\\ \sin m\varphi\end{bmatrix}}{J_m[x'_{mn}]\sqrt{x'^2_{mn}-m^2}} \cdot\sqrt{\frac{2}{\pi(1+\delta_{0m})}} \tag{5b}$$

which are suitably normalized, so that the power carried by each mode is 1 W for propagating modes, jW for evanescent TE modes, $-jW$ for evanescent TM modes [10, [29], [30].

In (2)–(5), the usual abbreviations [32] are chosen: k_x, k_y are the separation constants of the rectangular waveguide cross-section of the dimension a, b; k_c is the cutoff wavenumber; δ is the Kronecker symbol; J is the Besselfunction of the first kind; x_{ij} are the zeros of J; the prime denotes the derivative J' and its zeros x'_{mn}, respectively.

Matching the tangential electrical and magnetic field components, calculated by (1) and (2) results in the desired modal S-matrix of the key-building block discontinuity under investigation (Fig. 2(a))

$$\begin{bmatrix}\underline{b}^1\\ \underline{b}^2\end{bmatrix} = \begin{bmatrix}\underline{S}_{11} & \underline{S}_{12}\\ \underline{S}_{21} & \underline{S}_{22}\end{bmatrix}\cdot\begin{bmatrix}\underline{a}^1\\ \underline{a}^2\end{bmatrix}. \tag{6}$$

The submatrices of the modal S-matrix (6) are derived by the modified algorithm of [29], [30] which requires only the inversion of a submatrix with a quarter of the size of the original matrix of the coupling integrals. Moreover, the submatrix is advantageously merely of the order of the number of modes in the smaller waveguide section. The related coupling integrals are given in the Appendix.

For discontinuities of extreme step heights or widths, i.e. whenever the ratio of the step is more than about four, it may be advantageous to introduce artificial additional intermediate discontinuities of zero or extremely small lengths (cf. (Fig. 2(b)). This technique helps to reduce the overall number of modes required and to circumvent numerical instabilities which may otherwise often arise depending on the available number range of the used computer. For the dimensions x_s, y_s for the rectangular, or a_s of the circular waveguide intermediate sections of the subcascade, it has turned out that the geometric mean

$$x_s = \sqrt{x_1 x_2},$$
$$y_s = \sqrt{y_1 y_2};$$
$$a_s = \sqrt{a_1 a_2}, \tag{7}$$

of the corresponding geometrical step dimensions is a good choice, where the lengths l_S for the intermediate sections may be chosen to be zero (or a small value, like about 1 μm). For the rectangular-to-circular waveguide transition, the intermediate sections may be either rectangular or circular waveguide sections.

For calculating the discontinuity from a large circular to a small rectangular waveguide (like for the filter type of Fig. 1(f)), we introduce advantageously an intermediate square-waveguide region of zero length with the sidelength equal to the diameter of the circular waveguide. A direct calculation of the discontinuity would require a weighted sum of Bessel functions to approximate the vanishing tangential electric field on the metallic surface in the discontinuity plane. Due to the poor convergence performance of these functions, this might be a difficult problem as far as the numerical evaluation on

a computer is concerned. By introducing the intermediate square-waveguide region, this problem is elegantly avoided since now the inverse condition—zero tangential electric field on the metallic surface between a larger rectangular to a smaller circular waveguide—can be satisfied by a superposition of sine and cosine functions.

For composite structures, the direct combination of the corresponding modal S-matrices of all key-building block step discontinuities and of the intermediate homogeneous waveguide sections between them is used [10], [21], [29], [30], [32]. The submatrices of the modal S-matrices may be of unsymmetrical order (m, n) (i.e. unsymmetrical number of ports, or modes considered at the ports), and only one matrix inversion of size $n \cdot n$ is required.

Although we investigated the admittance matrix combining technique [35] as well, the generalized S-matrix technique [10] was preferred here. It has turned out that the computational effort for this kind of application is nearly the same for both techniques, as a very different number of localized and accessible modes [8] has advantageously been chosen in each subregion which requires also matrix inversions for the case of reduced admittance matrices [35].

A computer program was written using the preceding relations and utilizing the evolution strategy method [21], [29], [30] for optimizing the geometrical parameters. For an efficient computer-aided filter design, the computing time of the field theory optimization process have been reduced by applying the results of the conventional Cohn synthesis method [3] for the initial data.

Comprehensive investigations have been carried out to state an adequate compromise between the convergence behavior and cpu time required as a function of the modes taken into account for the field theory modeling of the geometrical structures in this paper. The criteria were the verification with measurements of typical structures, on the one side, and a sufficient asymptotic behavior of the S-parameter values within the interesting frequency range (e.g. by less than about 0.1%) as a function of the modes included, on the other side. This depends also largely on the absolute dimensions relative to wavelength or to the ratio of the discontinuity dimensions, cf. also the results reported in [16], [32]. As it would certainly be beyond the scope of this paper to present a more detailed description of these investigations, we hope that the following results may be sufficient to give the reader an adequate hint.

For rectangular waveguide rectangular iris filters, sufficient asymptotic behavior has been obtained by consideration of TE_{mn}- and TM_{mn}-modes up to $m = 5, n = 4$ in the resonator sections, and $m = 13, n = 4$ in the iris sections. The circular iris circular waveguide filters for TE_{11} mode excitation are calculated with higher order modes up to the order TE_{121}, TM_{121} in the larger, and TE_{115}, TM_{115} in the smaller circular waveguide sections. The corresponding modes for TE_{01} excitation are TE_{021}, and TE_{015}, respectively. For the rectangular waveguide filters with TE_{111} circular waveguide resonators, higher order modes have been chosen up to TE_{134}, TM_{134} in the rectangular waveguide section, TE_{121}, TM_{121}, TE_{312}, TM_{312}, TE_{58}, TM_{58}, in the circular waveguide resonator section; the corresponding modes in the smaller circular waveguide are chosen to be TE_{115}, TM_{115}, TE_{38}, $TM_{3,8}$, TE_{54}, TM_{54}.

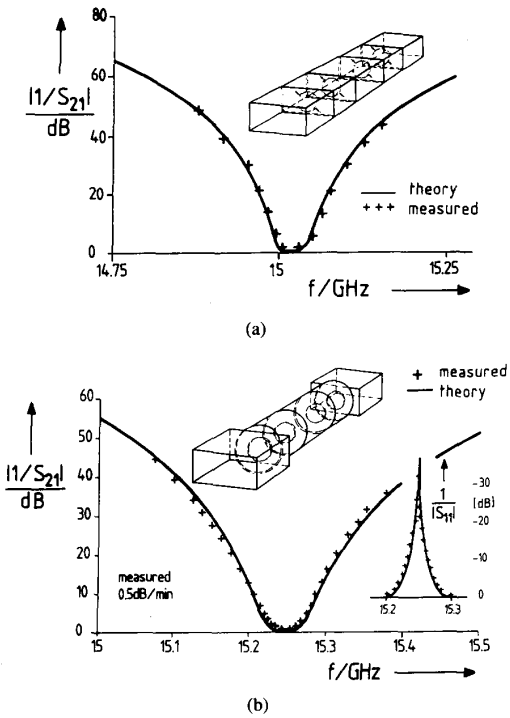

Fig. 3. Verification of the theory (—) with measurements (+++) (a) Computer-optimized circular iris coupled rectangular waveguide three-resonator filter. Filter dimensions are in mm (cf. Fig. 1(a)): $a = 15.8, b = 7.9, t = 0.218, a_1 = 2.577, a_2 = 1.142, a_3 = 1.125, a_4 = 2.592, l_1 = 12.499, l_2 = 12.819, l_3 = 12.461$. (b) Computer-optimized low-insertion loss circular iris coupled rectangular waveguide filter with three circular cavities. Filter dimensions in mm (cf. Fig. 1(d)): a = 15.8 mm, b = 7.9 mm, $a_0 = 6.985$ mm, $a_1 = 3.208$ mm, $a_2 = 1.695$ mm, $a_3 = 1.695$ mm, $a_4 = 3.205$ mm, $l_1 = 16.605$ mm, $l_2 = 17.219$ mm, $l_3 = 16.599$, $t = 0.192$mm.

III. Results

For the verification of the field-theory method described, Fig. 3 show the comparison between the measured results and the theoretically predicted values for a circular iris coupled rectangular waveguide three-resonator filter (Fig. 3(a)) and for a circular iris coupled rectangular waveguide filter with three circular cavities. Although the mechanical effort for the construction of the filter in Fig. 3(b) is higher, these filters achieve a lower insertion loss than those with rectangular waveguide resonators. Moreover, an utilization of mixed rectangular and circular waveguide elements offers the potential of increasing the spurious-free stopband by combining resonators with different spurious properties [33]. The excellent agreement between the computer-optimized and measured results in Fig. 3 demonstrates the efficiency of the design method described in this paper.

As rectangular waveguide filters may be manufactured by computer controlled techniques relatively easily and with high accuracy, this type of filters is considered to be attractive in the millimeter wave range, as well [36]. Although rectangular irises provide an additional degree of freedom (because of a

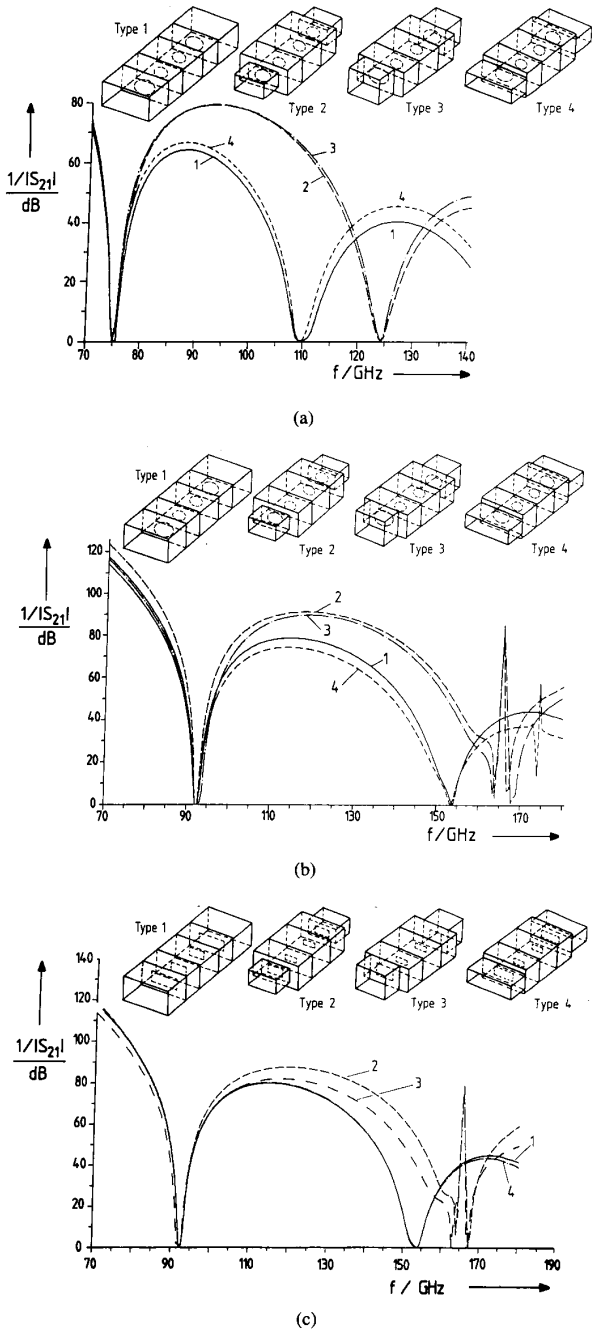

Fig. 4. Computer-optimized circular and rectangular iris coupled rectangular waveguide three-resonator filters with improved stopband. (a) Filters with passband near the lower end of the considered waveguide W-band (75 to 110 GHz). Circular irises. Filter dimensions cf. Table I. (b) Filters with passband about in the middle of the considered waveguide W-band. Circular irises. Filter dimensions cf. Table I. (c) Filters with passband about in the middle of the considered waveguide W-band. Rectangular irises. Filter dimensions cf. Table I.

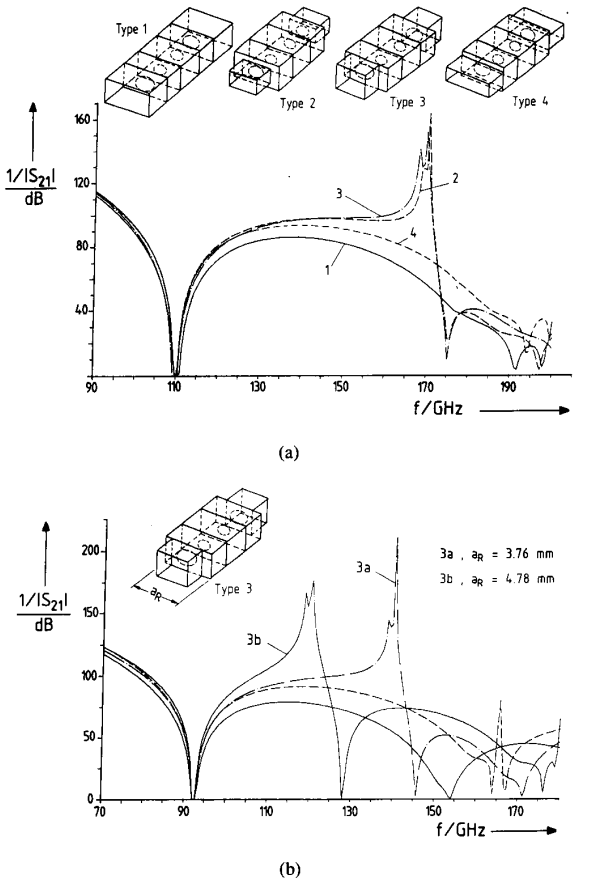

Fig. 5. Computer-optimized circular iris coupled rectangular waveguide three-resonator filters with stopband poles. Filter dimensions cf. Table I. (a) Filters with passband near the upper end of the considered waveguide W-band (b) Filters with passband near the middle of the considered waveguide W-band, optimized resonator a-dimension a_R. (Dashed curve: response of the filtertype 4.)

possible different choice of its a × b dimensions), circular irises are often preferred [14] as they may be fabricated more easily. It is demonstrated that nearly similar results may be achieved for circular iris coupled rectangular waveguide resonator filters than their rectangular iris coupled counterpart (cf. Figs. 4(b), 4(c)). Figs. 4, 5 present filters designed for the waveguide W-band (75–110 GHz, WR10 waveguide housing: 2.54 mm × 1.27 mm), for typically different pass-bands, i.e. near the middle (Fig. 4(b)–(c)), and near the lower (Fig. 4(a)) or upper end (Fig. 5(a)) of the waveguide band. The stopband behavior is included in the optimization process. If the size of the resonator section is suitably increased (type 2: WR12 housing: 3.10 mm × 1.55 mm; type 3: 3.10 mm × 1.27 mm) the stopband characteristic is significantly improved. This is mainly due to the lowered fundamental mode cutoff frequency of the resonator section which modifies advantageously the nonlinear relation between guide wavelength λ_g and frequency; the next resonance at about $2(\lambda_g/2)$ of the half-wave resonators, therefore tends towards higher frequencies. Filters of type 4 (Figs. 4(a)–5(a)) may be considered to confirm this fact because—though the resonator is increased—nearly the curve of type 1 is obtained since an increase in waveguide height does not alter the fundamental mode cutoff frequency. The dimensions of the filters in Figs. 4–9 are given in Table I.

TABLE I
FILTER DIMENSIONS IN FIGS. 4–9
(All dimensions in millimeters.)

Fig. 4(a)		(cf. Figs. 1 (a) and (b))		
Type 1:	$a = 2.5400$	$a_1 = 0.600$		$a_2 = 0.348$
	$b = 1.270$			
	$t = 0.050$		$l_1 = 2.986$	$l_2 = 3.162$
Type 2:	$a = 2.5400$	$a_R = 3.100$	$a_1 = 0.574$	$a_2 = 0.330$
	$b = 1.270$	$b_R = 1.550$		
	$t = 0.050$		$l_1 = 2.455$	$l_2 = 2.562$
Type 3:	$a = 2.5400$	$a_R = 3.100$	$a_1 = 0.548$	$a_2 = 0.286$
	$b = 1.270$	$b_R = 1.270$		
	$t = 0.050$		$l_1 = 2.458$	$l_2 = 2.574$
Type 4:	$a = 2.540$	$a_R = 2.540$	$a_1 = 0.624$	$a_2 = 0.396$
	$b = 1.2700$	$b_R = 1.550$		
	$t = 0.050$		$l_1 = 2.974$	$l_2 = 3.123$
Fig. 4(b)				
Type 1:	$a = 2.540$		$a_1 = 0.476$	$a_2 = 0.261$
	$b = 1.270$		$l_1 = 1.977$	$l_2 = 2.071$
	$t = 0.050$			
Type 2:	$a = 2.540$	$a_R = 3.1000$	$a_1 = 0.452$	$a_2 = 0.227$
	$b = 1.270$	$b_R = 1.550$		
	$t = 0.050$		$l_1 = 1.825$	$l_2 = 1.883$
Type 3:	$a = 2.5400$	$a_R = 3.1000$	$a_1 = 0.475$	$a_2 = 0.268$
	$b = 1.2700$	$a_R = 1.2700$		
	$t = 0.0500$		$l_1 = 1.784$	$l_2 = 1.855$
Type 4:	$a = 2.5400$	$a_R = 2.5400$	$a_1 = 0.504$	$a_2 = 0.288$
	$b = 1.2700$	$b_R = 1.5500$		
	$t = 0.0500$		$l_1 = 1.975$	$l_2 = 2.069$
Fig. 4(c)				
Type 1:	$a = 2.5400$		$a_1 = 0.742$	$a_2 = 0.4772$
	$b = 1.2700$		$b_1 = 1.0937$	$b_2 = 0.3603$
	$t = 0.0500$		$l_1 = 1.9812$	$l_2 = 2.0768$
Type 2:	$a = 2.5400$	$a_R = 3.100$	$a_1 = 0.7496$	$a_2 = 0.4286$
	$b = 1.2700$	$b_R = 1.5500$	$b_1 = 0.8468$	$b_2 = 0.3878$
	$t = 0.050$		$l_1 = 1.8201$	$l_2 = 1.8772$
Type 3:	$a = 2.540$	$a_R = 3.100$	$a_1 = 0.7279$	$a_2 = 0.3533$
	$b = 1.270$	$b_R = 1.2700$	$b_1 = 0.9141$	$b_2 = 0.6335$
	$t = 0.050$		$l_1 = 1.8125$	$l_2 = 1.8764$
Type 4:	$a = 2.5400$	$a_R = 2.5400$	$a_1 = 0.7370$	$a_2 = 0.4712$
	$b = 1.270$	$b_R = 1.550$	$b_1 = 1.2283$	$b_2 = 0.4631$
	$t = 0.050$		$l_1 = 1.9935$	$l_2 = 2.0708$
Fig. 5(a)				
Type 1:	$a = 2.540$		$a_1 = 0.389$	$a_2 = 0.186$
	$b = 1.270$		$l_1 = 1.545$	$l_2 = 1.599$
	$t = 0.050$			
Type 2:	$a = 2.540$	$a_R = 3.100$	$a_1 = 0.396$	$a_2 = 0.184$
	$b = 1.270$	$b_R = 1.550$	$l_1 = 1.465$	$l_2 = 1.506$
	$t = 0.050$			
Type 3:	$a = 2.540$	$a_R = 3.100$	$a_1 = 0.408$	$a_2 = 0.197$
	$b = 1.270$	$b_R = 1.270$	$l_1 = 1.450$	$l_2 = 1.503$
	$t = 0.050$			
Type 4:	$a = 2.540$	$a_R = 2.540$	$a_1 = 0.418$	$a_2 = 0.242$
	$b = 1.270$	$b_R = 1.550$	$l_1 = 1.531$	$l_2 = 1.583$
	$t = 0.050$			
Fig. 5(b)				
Type 3a:	$a = 2.540$	$a_R = 3.760$	$a_1 = 0.4914$	$a_2 = 0.350$
	$b = 1.270$	$b_R = 1.270$	$l_1 = 1.953$	$l_2 = 1.995$
	$t = 0.050$			
Type 3b:	$a = 2.540$	$a_R = 4.780$	$a_1 = 0.410$	$a_2 = 0.184$
	$b = 1.270$	$b_R = 1.270$	$l_1 = 1.673$	$l_2 = 1.711$
	$t = 0.050$			
Fig. 6(a)				
	$a = 15.8$		$a_1 = 2.29$	$a_2 = 0.955$
	$b = 7.9$	$t = 0.2$	$l_1 = 10.801$	$l_2 = 11.062$
Fig. 6(b)				
	$a = 7.112$	$a_R = 9.392$	$a_1 = 1.70$	$a_2 = 1.224$
	$b = 3.556$	$b_R = 3.556$	$l_1 = 6.382$	$b_2 = 2.377$
	$t = 0.19$			$l_2 = 6.78$
Fig. 7				
	$a = 15.8$	$a_1 = 3.913$	$a_2 = 2.222$	$s_2 = 1.687$
	$b = 7.9$	$l_1 = 11.217$	$l_2 = 12.516$	$l_3 = 12.686$
	$t = 0.2$			
		$a_4 = 1.569$		$l_4 = 12.712$
Fig. 8(a):				
	$a_0 = 16.269$		$a_1 = 6.718$	$a_2 = 3.888$
	$t = 0.2$		$l_1 = 10.907$	$l_2 = 11.142$
Fig. 8(b)				
solid line:				
	$a = 2.54$	$a_R = a$	$a_1 = 0.5$	$l_1 = 1.951$
	$b = 1.27$	$b_R = 0.5$	$c_1 = 0.5$	$d_1 = 0.2473$
dashed line:				
	$a = 2.54$	$a_R = a$	$a_1 = 0.5$	$l_1 = 1.951$
	$b = 1.27$	$b_R = b$		
Fig. 9 (cf. Fig. 1(f)):				
	$a_0 = 6.985$		$a_1 = 2.596$	$a_2 = 1.769$
	$t = 0.19$		$b_1 = 7.409$	$b_2 = 3.343$
			$l_1 = 14.580$	$l_2 = 15.056$

Dual mode resonance effects of the fundamental and the next higher-order mode (in this case TE_{30}) in suitably increased resonators may be utilized to improve the edge steepness and the stopband characteristic [34]. This is demonstrated for circular iris coupled filters in Fig. 5(a) where the TE_{30} cutoff frequency of the increased resonators of the type 2, 3 filters is given by about 145 GHz. This feature may also be applied for filter designs of improved edge steepness for lower passbands (Fig. 5(b)) by suitably optimized resonator sections: Type 3a utilizes an optimized a_R-dimension of a = 3.76 mm (i.e. $f_{c\mathrm{TE30}} \simeq 119.7$ GHz), for type 3b, $a_R = 4.78$mm is obtained ($f_{c\mathrm{TE30}} \simeq 94$ GHz).

The characteristic of a computer-optimized Ku-band (WR62 housing:15.8 mm × 7.9 mm) circular iris coupled three-resonator rectangular waveguide filter is presented in Fig. 6(a). Good rejection quality is obtained including the whole adjacent waveguide K-band (18–26 GHz). In order to demonstrate the possibility of a mixed iris design, a Ka-band filter (WR28 housing: 7.112 mm × 3.556 mm) with mixed circular and rectangular iris coupling and additionally optimized resonator width ($a_R = 9.392$ mm) is shown in Fig. 6(b). Although the passband of the filters is designed for about 27 GHz

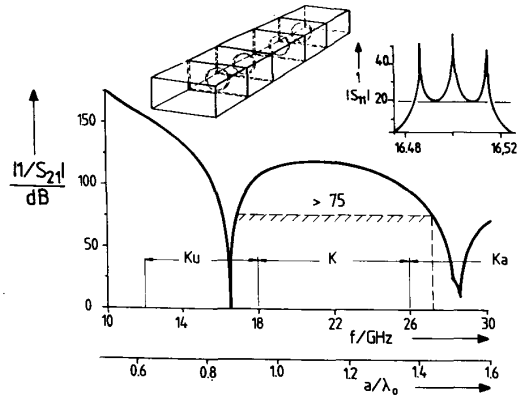

(a)

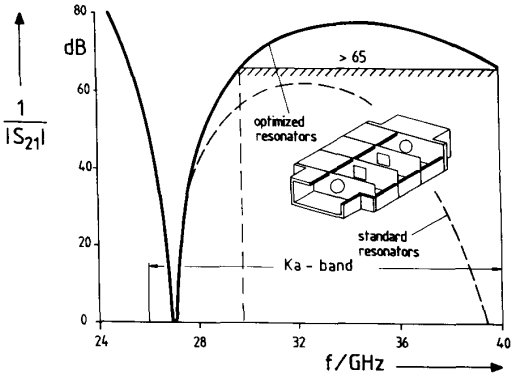

(b)

Fig. 6. Computer-optimized three-resonator rectangular waveguide filter with improved stopband. Filter dimensions cf. Table I (a) Circular iris coupled narrow-band filter. (b) Mixed circular and rectangular iris coupled filter with optimized resonator dimensions (solid line) and standard resonator dimensions (dashed line).

(i.e. near the beginning of the Ka-band, 26–40 GHz), a stopband attenuation of more than 65 dB is obtained within the whole Ka-band, whereas its conventional counterpart (WR28 resonators, rectangular irises) yields only a relatively poor stopband characteristic.

Fig. 7 presents the results of a circular iris coupled seven rectangular waveguide resonator filter in the Ku-band (WR62 housing: 15.8 mm × 7.9 mm). The initial values for the design optimization have been computed by the conventional Cohns' synthesis method [3] together with the iris impedances of [14]. The total cpu time for optimizing the filter was about 5 hours on a standard low-cost IBM RISC 6000 workstation (model 320). For this filter example in Fig. 7 with pure circular irises, the relatively low bandwidth of about 1\% could not be increased (cf. the return loss figure where some of the possible poles are out-of-band). This is because of the fact, that the optimized first circular iris diameter $2a_1 = 7.826$ mm has already attained to the fabrication limit of $b = 7.9$ mm (i.e. the waveguide height), cf. Table I. The design potential, therefore, for ths special example is exhausted. The filter characteristic may be improved (not shown here), however, by utilizing

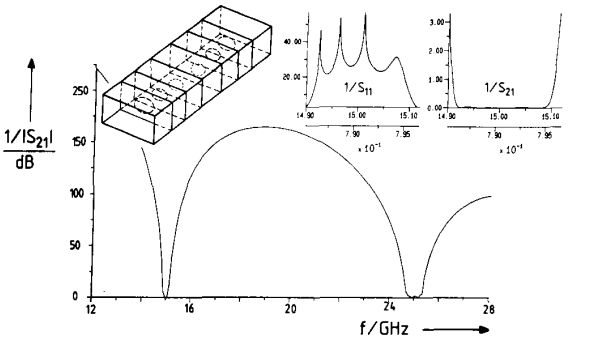

Fig. 7. Computer-optimized circular iris coupled seven-resonator rectangular waveguide filter. Filter dimensions cf. Table I.

mixed irises, cf. Fig. 1(c), where the first iris a × b dimensions offer a more extended design potential.

At this place we would like to note that for such symmetric structures, the TE_{20}-mode is not excited and, hence, is not considered in Fig. 7. Spurious responses due to asymmetric TE_{20}-mode interference (e.g. excited by slightly unsymmetrical structures owing to fabrication errors) occasionally reported by practitioners may be included in the field theory design if the realistic dimensions of the fabricated filter are taken into account.

The characteritics of computer-optimized circular iris coupled filters with additional stopband poles are presented in Figs. 8. Fig. 8(a) shows the behavior of a circular waveguide TE_{01}-mode three-resonator filter (as a function of the real and normalized frequency, since the results may be scaled up easily to an arbitrary waveguide band). Due to the interactions of the fundamental TE_{01} with the higher-order TE_{02} cavity mode, an improved stopband characteristic towards higher frequencies, together with high edge steepness, is achieved similar to the behavior of an elliptic function filter [28]. It should be noted, however, that it is very difficult in practice to excite a clean TE_{01} -mode. Moreover the degenerate TM_{01}-mode presents notoriously serious problems in these types of filters.

Fig. 8(b) shows the results of one-resonator filters designed for a pass-band at about 94 GHz. The asymmetric iris type (bold line) utilizes the interactions between the fundamental TE_{10} and the next higher TE_{20} cavity mode to achieve an additional stopband pole. The comparison with a conventional symmetric filter (thin line) of nearly the same passband characteristic demonstrates the improvement of the stopband

For some applications, rectagular-iris coupled circular waveguide filters are preferred [27] over rectangular resonator sections due to lower losses and the possibility of dual-mode operation. Such designs can be included in our theory as it is demonstrated in Fig. 9 at the example of a three-resonator circular waveguide Ku-band filter with rectangular irises. As already mentioned, for the calculation, advantageously an appropriate artificial intermediate quadratic waveguide section (dimension $a = b = 2a_0$, i.e. of the inner diameter the circular waveguide resonator) of zero length has been added at each circular-to-rectangular waveguide discontinuity. For this type of filters, again the problem of degenerate modes may occur

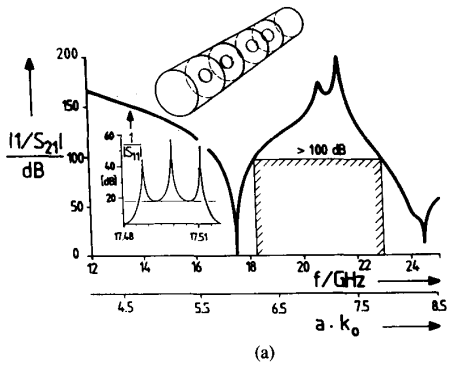

(a)

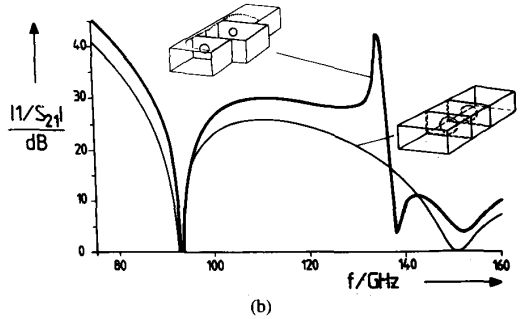

(b)

Fig. 8. Computer-optimized waveguide filters with stopband poles. Filter dimensions cf. Table I. (a) Circular waveguide TE $_{01}$-mode three-resonator filter. (b) Rectangular waveguide W-band (75–110 GHz) one-resonator filter (R900 housing, 2.54 mm × 127 mm) with symmetric (thin line) and asymmetric circular iris coupled resonators (bold line).

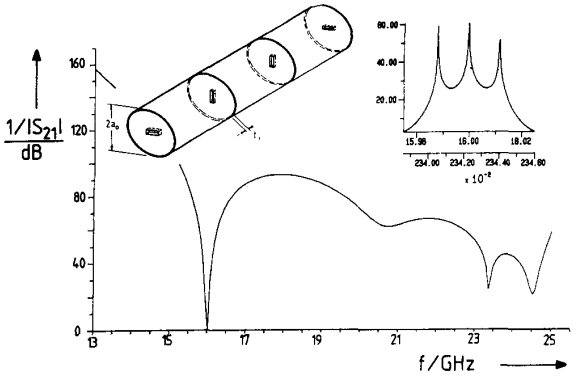

Fig. 9. Computer-optimized rectangular iris coupled three-resonator circular waveguide filter. Filter dimensions cf. Table I.

in practice. In this case, the TE_{111c}-circular-cavity-modes are degenerate with the orthogonal polarized TE_{111s}-modes. These effects can be included in the field theory design process if the realistic geometrical dimensions of the structures are adequately taken into account.

IV. Conclusion

The design theory described in this paper, which is based on the full wave mode-matching method for three key-building block elements associated with the generalized S-matrix technique for composite structures, achieves the rigorous computer-aided design of rectangular and circular waveguide filters coupled by rectangular and/or circular irises. Since the theory includes the finite iris thicknesses, the higher order mode interactions at all step discontinuities, as well as asymmetric structures, filters which may be arbitrarily composed of rectangular and circular waveguide elements can be rigorously designed by this method. Moreover, the stopband characteristic of the filters as well as the dimension of all additional step discontinuities are taken into account in the optimization process. Improved rejection characteristic is provided by cavities with modified geometry or by utilizing dual-mode resonance effects. The measured results verify the theory given by excellent agreement.

Appendix

Coupling Integrals of the Key Building Block (Fig. 2(a)

1) Coupling TE-to-TE

$$M^e_{[mn][kl]} =$$

$$\left(\frac{x'_{kl}}{a_2}\right)^2 \frac{4\sqrt{\frac{2}{\pi}}}{\sqrt{1+\delta_{0m}}\sqrt{1+\delta_{0n}}\sqrt{1+\delta_{0k}}\sqrt{a_1 b_1 k_c^1} J_k(x'_{kl})} \cdot \frac{1}{\sqrt{x'^2_{kl} - k^2}}$$

$$\left[\sum_{q=0}^{\infty} \frac{2(-1)^{2q}}{1+\delta_{02q}} \int_{\varphi=0}^{2\pi} \int_{r=0}^{a_2} J_{2q}(k_c^1 r) J_k\left(\frac{x'_{kl}}{a_2} r\right) r dr \cdot [\cos 2q\alpha \cos 2q\varphi \cos k'_x c_1 \cos k_y^1 d_1 - \sin 2q\alpha \sin 2q\varphi \sin k_x^1 c_1 \sin k_y^1 d_1] \cdot \begin{pmatrix} \cos k\varphi \\ \sin k\varphi \end{pmatrix} d\varphi + \sum_{q=0}^{\infty} 2(-1)^{2q+1} \int_{\varphi=0}^{2\pi} \int_{r=0}^{a_2} j_{2q+1}(k_c^1 r) J_k\left(\frac{x'_{kl}}{a_2} r\right) r dr \cdot [\cos(2q+1)\alpha \cos(2q+1)\varphi \sin k_x^1 c_1 \cos k_y^1 d_1 + \sin(2q+1)\alpha \sin(2q+1)\varphi \cos k_x^1 c_1 \sin k_y^1 d_1] \cdot \begin{pmatrix} \cos k\varphi \\ \sin k\varphi \end{pmatrix} d\varphi \right],$$

where x_{kl}, x'_{kl} are the lth root of the Besselfunction$J_k(x)$, or its derivative $J'_k(x)$, respectively;δ_{0n} is the Kronecker delta; k_c^1 is the cut-off wavenumber in region 1 (Fig. 2(a)); k_x^1, k_y^1 are$(q\pi/a_1), (q\pi/b_1)$, respectively; and the relation holds

$$\frac{\sin\alpha}{\cos\alpha} = \tan\alpha = \frac{k_x^1}{k_y^1}.$$

2) Coupling TM-to-TM

$$M^e_{(ij)(op)} =$$

$$\frac{4(k_c^1)^2}{\sqrt{a_1 b_1 k_c^1}} \sqrt{\frac{2}{\pi(1+\delta_{0o})}} \frac{1}{J'_o(x_{op}) x_{op}} \cdot \left[\sum_{q=0}^{\infty} \frac{2(-1)^{2q}}{1+\delta_{02q}} \int_{\varphi=0}^{2\pi} \int_{r=0}^{a_2} J_{2q}(k_c^1 r) J_0\left(\frac{x_{op}}{a_2} r\right) r dr\right.$$

$$\cdot [\cos 2q\alpha \cos 2q\varphi \sin k_x^1 c_1 \sin k_y^1 d_1 - \sin 2q\alpha \sin 2q\varphi \cos k_x^1 c_1 \cos k_y^1 d_1] \cdot \begin{pmatrix} \cos o\varphi \\ \sin o\varphi \end{pmatrix} d\varphi + \sum_{q=0}^{\infty} 2(-1)^{2q+1} \int_{\varphi=0}^{2\pi} \int_{r=0}^{a_2} J_{2q+1}(k_c^1 r) J_0\left(\frac{x_{op}}{a_2} r\right) r dr \cdot [\cos(2q+1)\alpha \cos(2q+1)\varphi \cos k_x^1 c_1 \sin k_y^1 d_1 + \sin(2q+1)\alpha \sin(2q+1)\varphi \sin k_x^1 c_1 \cos k_y^1 d_1] \cdot \begin{pmatrix} \cos o\varphi \\ \sin o\varphi \end{pmatrix} d\varphi \Bigg].$$

3) Coupling TM-to-TE

$$M^e_{(ij)[kl]} = \frac{-4}{\sqrt{a_1 b_1} k_c^1} \sqrt{\frac{2}{(1+\delta_{0k})}} \frac{1}{\sqrt{x'^2_{kl} - k^2}} \cdot \int_{\varphi=0}^{2\pi} \Bigg[\sum_{q=0}^{\infty} \frac{2(-1)^{2q}}{1+\delta_{02q}} J_{2q}(k_c^1 a_2) \cdot [\cos 2q\alpha \cos 2q\varphi \sin k_x^1 c_1 \sin k_y^1 d_1 - \sin 2q\alpha \sin 2q\varphi \cos k_x^1 c_1 \cos k_y^1 d_1] + \sum_{q=0}^{\infty} 2(-1)^{2q+1} J_{2q+1}(k_c^1 a_2) \cdot [\cos(2q+1)\alpha \cos(2q+1)\varphi \sin k_x^1 c_1 \cos k_y^1 d_1 + \sin(2q+1)\alpha \sin(2q+1)\varphi \cos k_x^1 c_1 \sin k_y^1 d_1] \Bigg] \cdot \begin{pmatrix} -k \cos k\varphi \\ -k \sin k\varphi \end{pmatrix} d\varphi.$$

4) The Coupling TM-to-TE is zero (like for the rectangular waveguide double step discontinuity [10])

REFERENCES

[1] H. A. Bethe, "Theory of diffraction by small holes," *Phys. Rev.*, vol. 66, pp. 163–182, Oct. 1944.

[2] N. Marcuvitz, *Waveguide Handbook*. New York: McGraw-Hill, 1951.

[3] G. Matthaei, L. Young, and E. M. T. Jones, *Microwave Filters, Impedance-Matching Networks, and Coupling Structures*. New York: McGraw-Hill, 1964.

[4] S. B. Cohn, "Microwave coupling by large apertures," *Proc. IRE*, vol. 40, pp. 696–699, June 1972.

[5] N. A. McDonald, "Electric and magnetic coupling through small apertures in shielded walls of any thicknesses," *IEEE Trans. Microwave Theory Tech.*, vol. MTT-20, pp. 689–695, Oct. 1972.

[6] R. J. Luebbers and B. A. Munk, "Analysis of thick rectangular waveguide windows with finite conductivity," *IEEE Trans. Microwave Theory Tech.*, vol. MTT-21, pp. 461–468, July 1973.

[7] R. Levy, "Improved single and multiaperture waveguide coupling theory, including explanation of mutual interactions," *IEEE Trans. Microwave Theory Tech.*, vol. MTT-28, pp. 331–338, Apr. 1980.

[8] M. S. Navarro, T. E. Rozzi, and Y. Z. Lo, "Propagation in a rectangular waveguide periodically loaded with resonant irises," *IEEE Trans. Microwave Theory Tech.*, vol. MTT-28, pp. 857–865, Aug. 1980.

[9] H. D. Knetsch, "Wellentypwandler und Filter mit Rechteck- und Rundhohlleiterelementen," *Nachrichtentechnische Zeitschrift*, NTZ - 23, p. 57–63, Feb. 1970.

[10] H. Patzelt and F. Arndt, "Double-plane steps in rectangular waveguides and their application for transformers, irises, and filters," *IEEE Trans. Microwave Theory Tech.*, vol. MTT-30, pp. 771–776, May 1982.

[11] R. Savafi-Naini and R. H. MacPhie, "Scattering at rectangular-to-rectangular waveguide junctions," *IEEE Trans. Microwave Theory Tech.*, vol. MTT-30, pp. 2060–2063, Nov. 1982.

[12] T. S. Chen, "Characteristics of waveguide resonant-iris filters," *IEEE Trans. Microwave Theory Tech.*, vol. MTT-15, pp. 260–262, Apr. 1967.

[13] H. L. Thal, "Transmit-receive multiplexer for the 12–14-GHz Band," *IEEE Trans. Microwave Theory Tech.*, vol. MTT-30, pp. 1324–1330, Sept. 1982.

[14] A. Jennings and R. L. Gray, "Extension of Levy's large-aperture design formulas to the design of circular irises in coupled-resonator waveguide filters," *IEEE Trans. Microwave Theory Tech.*, vol. MTT-23, pp. 1489–1493, Nov. 1984.

[15] R. Levy, "Theory of direct coupled-cavity filters," *IEEE Trans. Microwave Theory Tech.*, vol. MTT-15, pp. 340–348, June 1967.

[16] Y. C. Shih and K. G. Gray, "Convergence of numerical solutions of step-type waveguide discontinuity problems by modal analysis," in *1983 IEEE MTT-S Int. Symp. Dig.*, pp. 233–235.

[17] J. D. Wade and R. H. MacPhie, "Scattering at circular-to-rectangular waveguide junctions," *IEEE Trans. Microwave Theory Tech.*, vol. MTT-34, pp. 1085–1091, Nov. 1986.

[18] R. W. Scharstein and A. T. Adams, "Thick circular iris in a TE $_{11}$ mode circular waveguide," *IEEE Trans. Microwave Theory Tech.*, vol. MTT-36, pp. 1529–1531, Nov. 1988.

[19] F. Arndt, J. Dittloff, U. Papziner, D. Fasold, N. Nathrath, and H. Wolf, "Rigorous field theory design of compact and lightweight broadband diplexers for satellite communication systems," in *Proc. European Microwave Conf.*, London, Sept. 1989, pp. 1214–1219.

[20] J. Bornemann and R. Vahldieck, "Characterization of a class of waveguide discontinuities using a modified TE$^z_{mn}$ mode approach," *IEEE Trans. Microwave Theory Tech.*, vol. 38, pp. 1816–1822, Dec. 1990.

[21] F. Arndt *et al.*, "Modal-S-matrix method for the optimum design of inductively direct-coupled cavity filters," *Proc. Inst. Elec. Eng.*, vol. 133, Pt. H, pp. 341–350, 1986.

[22] W. Hauth, R. Keller, and U. Rosenberg, "CAD of waveguide low-pass filters for satellite applications," in *Proc. European Microwave Conf.*, Rome, Sept. 1987, pp. 151–156.

[23] R. E. Collin, *Field Theory of Guided Waves*. New York: McGraw-Hill, 1960.

[24] G. B. Eastham and K. Chang, "Analysis of circular and rectangular apertures in a circular waveguide," in *IEEE MTT-S Int. Symp. Dig.*, pp. 263–266, 1990.

[25] S. B. Cohn, "Direct-coupled cavity filters," *Proc. IRE*, vol. 45, pp. 187–196, 1957.

[26] L. Young, "Direct-coupled cavity filters for wide and narrow bandwidths," *IEEE Trans. Microwave Theory Tech.*, vol. MTT-11, pp. 162–178, 1963.

[27] E. Atia and A. E. Williams, "Narrow-bandpass waveguide filters," *IEEE Trans. Microwave Theory Tech.*, vol. MTT-20, pp. 258–265, Apr. 1972.

[28] S. J. Fiedziuszko, "Dual-mode dielectric resonator loaded cavity filters," *IEEE Trans. Microwave Theory Tech.*, vol. MTT-30, pp. 1311–1316, Sept. 1982.

[29] J. Dittloff and F. Arndt, "Rigorous field theory design of millimeter-wave E-plane integrated circuit diplexers," *IEEE Trans. Microwave Theory Tech.*, vol. 37, pp. 335–350, Feb. 1989.

[30] J. Bornemann and F. Arndt, "Modal-S-matrix design of optimum stepped ridged and finned waveguide transformers," *IEEE Trans. Microwave Theory Tech.*, vol. MTT-35, pp. 561–567, June 1987.

[31] G. L. James, "Analysis and design of TEW$_{11}$-to-HE $_{11}$ corrugated cylindrical waveguide mode converters," *IEEE Trans. Microwave Theory Tech.*, vol. MTT-29, pp. 1059–1066, Oct. 1981.

[32] F. Arndt, U. Tucholke, and T. Wriedt, "Computer-optimized multisection transformers between rectangular waveguides of adjacent frequency bands," *IEEE Trans. Microwave Theory Tech.*, vol. MTT-32, pp. 1479–1484, Dec. 1974.

[33] H. J. Riblet, "Waveguide filter having nonidentical sections resonant at same fundamental and different harmonic frequencies," US Patent No. 3,153,208, 1964.

[34] F. Arndt, T. Duschak, U. Papziner, and P. Rolappe, "Asymmetric iris coupled cavity filters with stopband poles," in *IEEE MTT-S Int. Symp. Dig.*, pp. 215–218, 1990.

[35] F. Alessandri, G. Bartolucci, and R. Sorrentino, "Admittance matrix formualtion of waveguide discontinuity problems: Computer-aided design of branch guide couplers," *IEEE Trans. Microwave Theory Tech.*, vol. 36, pp. 394–403, Feb. 1988.

[36] R. V. Snyder, "All the world is a filter," *IEEE MTT Newsletter*, no. 127, pp. 5–10, Fall 1990.

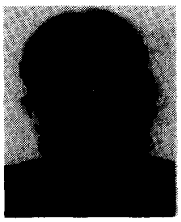

Fritz Arndt (SM'83–F'93) received the Dipl. Ing., Dr. Ing., and Habilitation degrees from the Technical University of Darmstadt, Germany, in 1963, 1968, and 1972, respectively.

From 1963 to 1972, he worked on directional couplers and microstrip techniques at the Technical University of Darmstadt. Since 1972, he has been a Professor and Head of the Microwave Department of the University of Bremen, Germany. His research activities are in the area of the solution of field problems of waveguide, finline, and optical waveguide structures, of antenna design, and of scattering structures.

Dr. Arndt is a member of the VDE and NTG (Germany). He received the NTG award in 1970, the A. F. Bulgin Award (together with three coauthors) from the Institution of Radio and Electronic Engineers in 1983, and the best paper award of the antenna conference JINA 1986 (France).

Uwe Papziner was born in Delmenhorst, West Germany, on January 18, 1961. He received the Dipl.-Ing. and Dr.-Ing. degrees in electrical engineering from the University of Bremen in 1986 and 1990, respectively. From 1986 to 1990 he worked on waveguide filter, diplexer, taper and horn antenna design problems.

Since 1990 he has been working at Atlas Elektronik GmbH in Bremen as a research engineer, in the field of acoustic waves and Ground Penetrating Radar.